

## **Strengthening of Continuous Beams Using Fiber Reinforced Polymer Laminates**

**by N. F. Grace, A. K. Soliman, G. Abdel-Sayed, and K. R. Saleh**

### **Synopsis:**

The use of fiber reinforced polymers (FRP) to strengthen sagging and hogging moment regions of continuous beams is discussed in this paper. Five two-span reinforced concrete beams with "T" cross sections were tested. Four different strengthening systems were examined. Two beams were strengthened with two different types of carbon fiber reinforced polymer (CFRP) sheets. The first beam was strengthened for flexure only while the second beam was strengthened for both flexure and shear. The third beam was strengthened with glass fiber reinforced polymer (GFRP) sheets, while CFRP plates were used in strengthening the fourth beam. The fifth beam was a control. Each beam was loaded and unloaded for at least one cycle of loading before failure. The effects of FRP strengthening on failure modes, load capacity, cracking pattern and propagation, and deflections are presented. It was concluded that the use of FRP laminates to strengthen continuous beams is effective in reducing deflections and increasing their load carrying capacity. Furthermore, beams strengthened with FRP laminates exhibit smaller and better-distributed cracks.

**Keywords:** carbon; continuous beam; failure mode; fiber; flexural; glass; laminates; shear; strengthening

**Nabil F. Grace** is a professor of the Civil Engineering Department at Lawrence Technological University, Southfield, Michigan. His current research interests are in the use of FRP in reinforced and prestressed concrete bridges and in strengthening deficient structures.

**Ahmed K. Soliman** is a professor of the Civil Engineering Department at the Suez-Canal University, Port-Said, Egypt. His research focuses on the analysis and the behavior of reinforced and prestressed concrete structures.

**George Abdel-Sayed** is an Emeritus professor of the Civil and Environmental Engineering Department, University of Windsor, Windsor, Ontario, Canada.

**Khaled R. Saleh** is research assistant and Ph.D. candidate of the Civil Engineering Department at Lawrence Technological University, Southfield, Michigan. His research work deals with the use of FRP in reinforced concrete structures.

## INTRODUCTION

Strengthening is the economical solution for extending the life of deficient structures. The optimum strengthening method and material used should not add dead load or reduce beam clearance. Steel plates bonded onto beam surfaces provide a very efficient solution for indoor applications. However, in outdoor applications, traces of corrosion have been observed, which can destroy the bonding between the plates and the concrete. Because of handling considerations, the length of the plates is limited, especially when mechanical facilities cannot be used. Fiber reinforced polymer (FRP) laminates are superior to steel plates in that they offer high resistance to electrochemical corrosion, a high strength to weight ratio, ease of handling, the ability to be formed to any shape, fatigue resistance, and are available in any length. The strengthening of simple beams using FRP laminates has been recently studied and has found its way to several field applications in Europe, Japan and North America [1]. Extensive literature survey suggested that little work has been carried out in order to examine the feasibility of using these materials in strengthening continuous beams. Arduini et. al [2] investigated the strengthening of five continuous beams (three were shallow and two were deep beams). They used CFRP sheets to strengthen the flexural areas of the shallow beams, and both the flexural and shear areas of the deep beams.

## EXPERIMENTAL WORK

Five continuous beams with T cross-sections were constructed, strengthened, and tested. Each beam had two equal spans of 3738 mm (12.25 ft). The web had a tapered shape of 101 mm (4.0 in.) at the flange to 76 mm (3.0 in.) at the bottom. The flange had a thickness of 50 mm (2.0 in.) and a width of 393 mm (15.5 in.).

The overall depth of the beam was 343 mm (13.5 in.). Each beam was reinforced with four 16 mm (#5) high tensile steel bars in the flange and two bars at the bottom of the web. The stirrups made of #3 bars were placed at 150 mm (6 in.) apart. The concrete used had a compressive strength of 48.2 MPa (7000 psi) and a typical slump of 200 mm (8 in.).

After curing, four beams were prepared for strengthening by sanding the two sides and the bottom surfaces, and rounding the two bottom corners of the webs. The test beams were not precracked prior to strengthening. Four commercially available strengthening systems (I-IV), shown in Table 1, were used in this study. Systems I and II are composed of unidirectional CFRP sheets of different thicknesses and strengths, while system III is composed of GFRP sheets. CFRP plates are used in system IV. Epoxy types 1, 2, and 3 were used with strengthening systems I, (II, III), and IV, respectively. Tables 2 and 3 show the characteristics of the strengthening laminates and epoxies, respectively. It should be pointed out that the sheets of strengthening system I have the highest mechanical properties in comparison to the other three strengthening systems.

Beam CF-I was strengthened using strengthening system I. Only the positive (sagging) and negative (hogging) moment regions were strengthened as shown in Fig. 1a. Beam CFS-II was strengthened using strengthening system II. The entire length of the two spans of this beam was strengthened, positive and negative moment regions, using one longitudinal layer as shown in Fig. 1b. In addition, the area of maximum shear at the middle support was strengthened with a U shaped layer. The fibers of this layer were running vertically. A U-shaped layer with the fibers oriented in the vertical direction was also attached to the longitudinal layer at each end support. These two vertical layers provided rings to anchor the longitudinal layers at their ends. It should be noted that the CFRP sheet of system II is twice as thick as the sheet of strengthening system I, as shown in Table 2.

Beam UG-III was prepared for strengthening in a manner similar to that used for beam CFS-II with the exception that every CFRP layer was replaced with two GFRP layers as shown in Fig. 1c. This beam was strengthened using system III with unidirectional GFRP sheets and epoxy type 2. It was necessary to double the number of layers when strengthening beam UG-III, since the tensile strength of the GFRP sheet is about half that of the CFRP sheet of system II. Furthermore, the modulus of elasticity of the GFRP sheet is only one-third that of the CFRP sheet of system II, as shown in Table 2. Beam CP-IV was strengthened using strengthening system IV. Two different widths of CFRP plates were used, namely, 50 and 80 mm (2.0 and 3.1 in.) wide plates. Both the flexural and shear regions were strengthened as shown in Fig. 1d. The positive and negative moment regions were strengthened using plates in the longitudinal direction while the shear region was strengthened using 60° oblique angle plates. It was thought that this arrangement would provide enough anchorage for the positive and negative moment strengthening plates. After resin curing, each

beam (including the control beam) was instrumented with dial gages, strain gages, load cells and string pots. Then, each beam was tested under two loads, one in the center of each span. The load in each span was applied simultaneously and in increments of 22.75kN (5 kips).

## DISCUSSION OF RESULTS

### 1. Deflections

Fig. 2 (a, b, c, d, and e) shows the load deflection relationships of the tested beams. Examining Fig 2 shows that the control beam had the largest deflection of all tested beams (279 mm (11 in.)), while beam CP-IV had the smallest deflection (137 mm (5.4 in.)). Furthermore, all beams but CP-IV exhibited linear load deflection relationships up to a load of 44.4 kN (10 kips). Beam CP-IV experienced a linear load deflection relationship up to a load of only 22.2 kN (5 kips); then a milder slope up to a load of 115.6 kN (26.0 kips). The presence of the FRP laminates precluded the flattening (yield) of the load-deflection curve, which was clear in the control beam between 124.5 and 146.8 kN (28 and 33 kips). Therefore, the laminates carried a portion of the tensile stresses, so that the steel reinforcing rods did not reach yield. As every beam failed at different load, the load of 89 kN (20 kips) was chosen to compare the deflections of the tested beams.

Two loading-unloading cycles were carried out during the testing of beam CF-I. The unloading was carried out at loads of 177.9 and 200.1 kN (40 and 45 kips), as shown in Fig. 2a. No significant difference in the stiffness of the beam was recorded during these two load cycles, as evident by the equality of the slopes of loading and unloading paths. These two loads represent 115 and 129% of the failure load of the control beam, indicating that the concrete was not severely cracked, and that the steel had not yielded under a load higher than the failure load of the unstrengthened beam. The deflections of the two mid-span sections were identical. At failure, the northern (right) and the southern (left) mid-span sections exhibited deflections of 150 and 160 mm (6.0 and 6.2in.), respectively. These deflections were 54 and 61%, respectively, of the deflection of the control beam. This reduction in deflection was accompanied by a 52% increase in failure load. Therefore, strengthening system I was effective in reducing beam deflection.

The load-deflection relationship of beam CFS-II was nearly tri-linear in the first loading cycle, (Fig. 2b), with changes in slope at 55.6 and 137.8 kN (12.5 and 31 kips). The beam was not cracked up to a load of 55.6 kN (12.5 kips). The reduction of stiffness due to cracking is the main source of the change in slope at that load. However, the increased reduction in stiffness after 137.8 kN (31 kips) is probably due to plastic deformation in the epoxy. In the second loading cycle, the-load-deflection relationship is nonlinear. The deflections at the two mid-spans were almost identical, suggesting the formation of symmetrical cracks in

each span. The maximum deflections at failure of the two mid-spans were 216 and 220 mm (8.5 and 8.7 in.), or 77 and 84% that of the control beam. These decreases in deflection were accompanied by a 33% increase in failure load, and were less than those of beam CF-I. This follows from the fact that the modulus of elasticity of the CFRP sheet of system I was 3.7 times that of the CFRP sheet of system II, as shown in Table 2. The maximum mid-span deflection was about 87% that of the control beam at a load of 89 kN (20 kips).

The load-deflection behavior of beam UG-III was identical to that of beam CFS-II up to a load of 22.2 kN (5 kips). After that, a multi-linear relationship was observed up to a load of 53.3 kN (12 kips). After 53.3 kN (12 kips), the load-deflection relationship was nonlinear, as shown in Fig. 2c. The deflections at the two mid-spans were not equal. The northern (right) mid-span section exhibited a deflection of 230 mm (9.0 in.), while the southern (left) mid-span exhibited a deflection of only 160 mm (6.3 in.). This difference can be attributed to unsymmetrical cracking in the two spans, as will be illustrated in Section 2.

The slope of the load-deflection relationship of beam CP-IV was identical to that of beam CFS-II up to a load of 22.2 kN (5 kips), as shown in Fig. 2d. Thereafter, this slope became much steeper than that of any other beam. The deflections at the two mid-spans were not equal. At failure, the northern (right) mid-span experienced a deflection of 210 mm (8.4 in.), while its southern counterpart had a deflection of only 120 mm (4.9 in.). Again, similar to beam UG-III, this difference in deflection can be attributed to unsymmetrical cracking in the two spans. In addition, the higher the load, the more pronounced is the effectiveness of strengthening system IV. For example, while a decrease in deflection of 6% was reported at a load of 89 kN (20 kips), a 24% decrease in deflection was reported at failure, which was accompanied by a 15% increase in load carrying capacity.

Fig. 2e shows the load deflection relationship of the control beam. Typical yielding of the steel reinforcement started at a load of 126 kN (28.5 kips). A relatively large residual deflection of 117 mm (4.6 in.) was the result of intensive cracking in the concrete. This residual deflection was almost double that of the strengthened beams, suggesting that a proper strengthening system can minimize the reduction of stiffness due to cracking.

### 2. Failure Loads and Modes

Figs. 3a shows the failed section of the control beam, which was traditional flexural failures at the maximum positive moment sections of the two mid-spans caused by yielding of the steel reinforcements.

Beam CF-I failed at a load of 235.7 kN (53 kips), which was 52% greater than the failure load of the control beam. At failure, only the CFRP fibers in the

southern mid-span section were ruptured, as shown in Fig. 3b. Localized crushing occurred in the high compressive stress zone immediately above the middle support, just before failure. This crushing was accompanied by 45° shear cracks extending from the middle support to the top of the beam. Since this beam was not strengthened for shear, the shear cracks extended underneath both the top and bottom CFRP sheets. However, no delamination of sheets occurred at these cracks.

Rupture of the CFRP sheets in beam CFS-II began at a load of 173.4 kN (39 kips), while complete failure occurred at a load of 206.8 kN (46.5 kips); a 33% increase over the control beam, as shown in Fig. 3c. The failure occurred in the two mid-span sections simultaneously. The failure of beam CFS-II was caused by the increase in tensile stress at the two load locations beyond the CFRP tensile strength, which caused horizontal and vertical ruptures in the sheets followed by concrete crushing in the flange at the mid-span sections. Therefore, unlike the failure of beam CF-I, the failure of beam CFS-II can not be described as a purely tensile failure. While horizontal ruptures were most significant at the northern mid-span, vertical ruptures which occurred exactly beneath the load at the southern mid-span were the most distinguishable. The horizontal ruptures of the northern mid-span were shifted toward the middle support near the failure load.

The rupture of the GFRP sheets in beam UG-III started at a load of 231.2 kN (52 kips). Complete failure occurred at a relatively high load of 258 kN (58 kips), a 66% increase in load carrying capacity over that of the control beam. This increase in load carrying capacity can be attributed to the use of two layers of GFRP sheets in the positive moment areas and four layers at the negative moment area. Similar to the failure of beam CFS-II, the failure of beam UG-III was caused by tensile flexural rupture of the sheets followed by crushing of concrete at the flange. However, failure occurred only in northern mid-span section, as shown in Fig. 12a. The GFRP sheets in the southern mid-span section did not experience any horizontal or vertical ruptures, as shown in Fig. 3d. The maximum negative moment area also experienced no rupture in the strengthening sheets no crushing of concrete, and no yielding of steel reinforcement bars.

Beam CP-IV failed at a load of 178 kN (40 kips), only a 15 percent increase in load carrying capacity over that of the control beam. The failure of this beam occurred simultaneously in the two spans, although with different maximum deflections. Failure was caused by “local” shear failure of concrete and simultaneous rupture of the diagonal plates, as shown in Fig. 3e. High flexural and shear stresses in the concrete resulted in the separation of the concrete cover below the lower reinforcements in the region of high interfacial stresses at the ends of the CFRP plates. This was not a delamination failure, as the CFRP plates were still bonded to the concrete and there was no failure in the bond.

## CONCLUSIONS

Five continuous beams were tested. Four beams were strengthened with four different FRP strengthening systems. It was concluded that using FRP laminates to strengthen continuous beams is effective in reducing deflections, increasing load capacity, and yielding smaller and better distributed cracks. However, the use of CFRP plates may lead to premature separation in the concrete cover. Furthermore, the strength of the CFRP plates used for shear strengthening at the middle support may not be fully developed due the lack of sufficient anchor length.

## REFERENCES

1. State-of-the-art of Composite Materials in Concrete Structures, ACI Committee No. 440, 1996, American Concrete Institute, Farmington Hills, Michigan.
2. Arduini, M., Nanni A., Di Tommaso, A., and Focacci, F., "Shear Response of Continuous RC Beams Strengthened with Carbon FRP sheets", Proceeding of the third international Symposium on Non-Metallic (FRP) Reinforcement for Concrete Structures, Sapporo, Japan, 1997, pp. 459-466.

**TABLE 1—FRP STRENGTHENING SYSTEMS.**

Strengthening System	I	II	III	IV
Type of Strengthening Material	CFRP*	CFRP*	GFRP*	CFRP#
Epoxy Type	1	2	2	3

\* Sheets

# Plates

TABLE 2—PROPERTIES OF STRENGTHENING LAMINATES.

Strengthening System	I	II	III	IV
Type of Fibers	CFRP	CFRP	GFRP	CFRP
Tensile Strength, Mpa (ksi)	2937 (426)	758 (110)	413 (60)	2399 (348)
Modulus of Elasticity, Gpa ( $\times 10^3$ ksi)	230 (33.4)	62 (9.0)	21 (3.0)	149 (21.7)
Failure Strain (%)	1.2	1.2	2.0	1.4
Thickness, mm ( $\times 10^{-1}$ ) (in.)	5 (0.02)	13 (0.05)	10 (0.05)	13 (0.05)

TABLE 3—PROPERTIES OF EPOXY.

Epoxy Type	1 epoxy resin	2 epoxy	3 epoxy adhesive
Tensile Strength, MPa (psi)	29.8 (4251)	66.5 (9500)	24.8 (3571)
Modulus of Elasticity, GPa (ksi)	--	2.7 (400)	4.5 (650)
Elongation at Break %	--	5	1
Shear Strength, MPa (psi)	9.8 (1391)	--	24.8 (3571)
Flexural Strength, MPa (psi)	39.2 (5700)	79.0 (11500)	46.8 (6771)



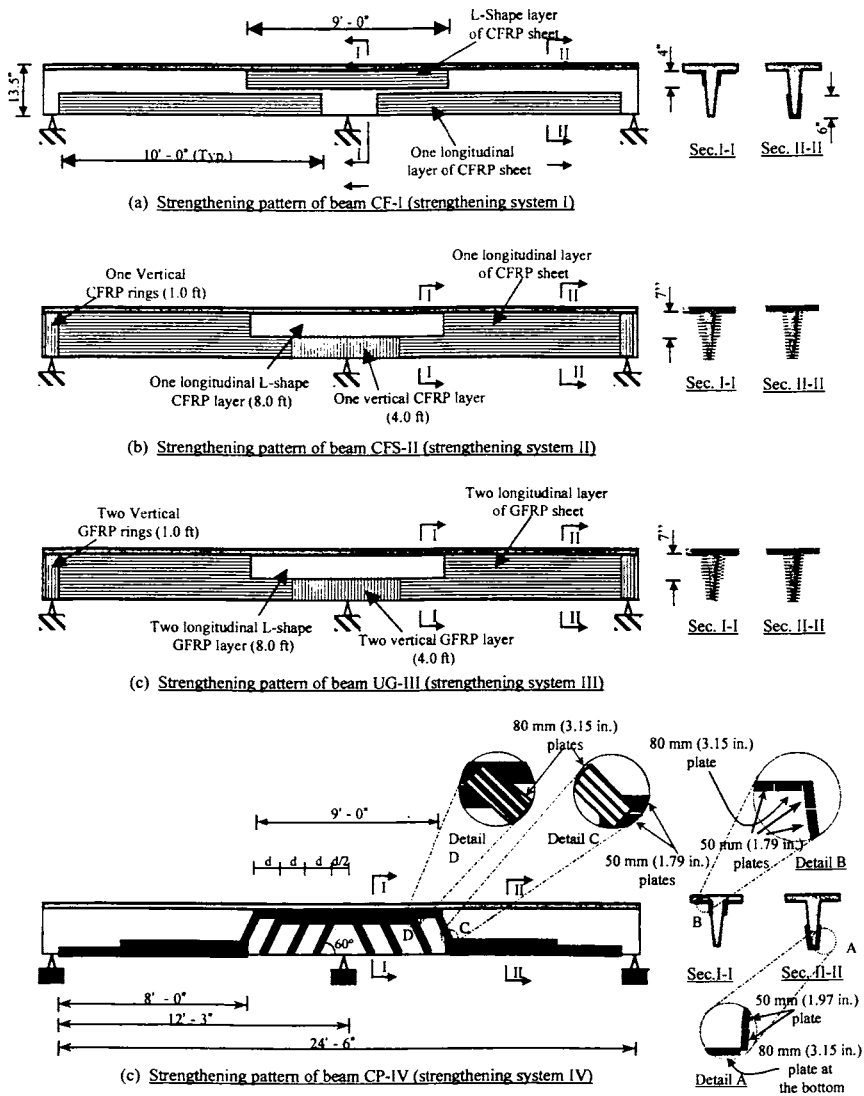


Fig. 1—Strengthening patterns of tested beams.

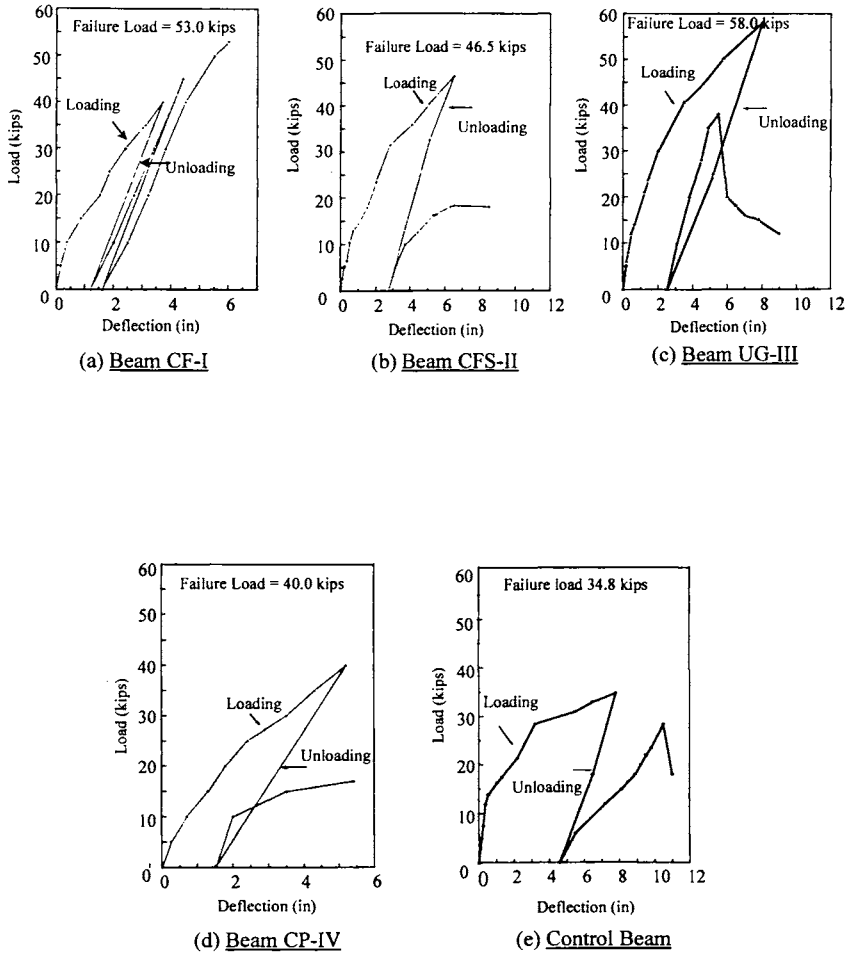
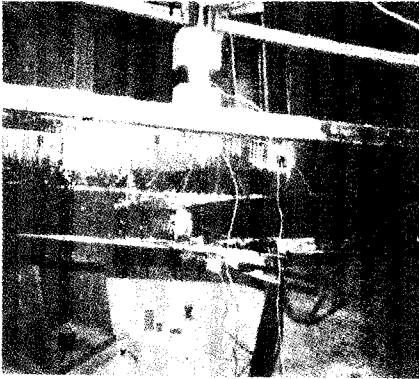


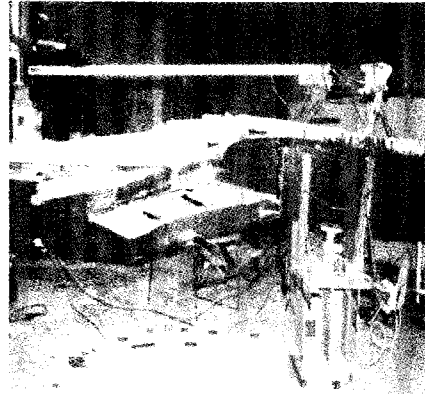
Fig. 2—Load-deflection behavior of tested beams.



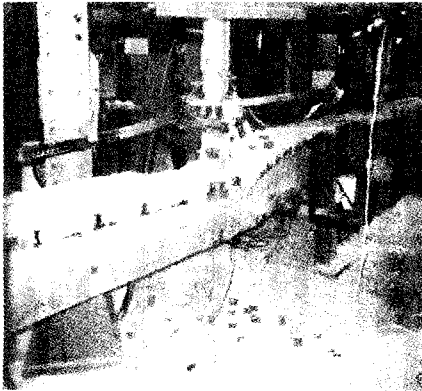
(a) Control beam



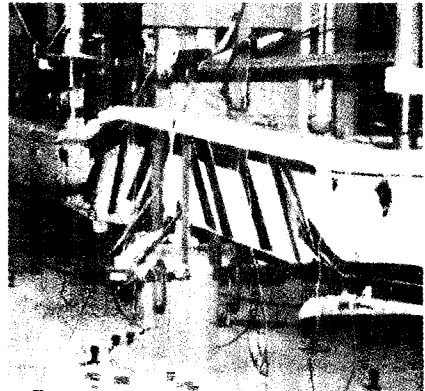
(b) Beam CF-I



(c) Beam CFS-II



(d) Beam UG-III



(e) Beam CP-IV

Fig. 3—Failure mechanism of strengthened beams.